ENDOCRINE
SOCIETY

OXFORD

Changes of FGF23 and the Renin-Angiotensin-System in Male Mouse Models of Chronic Kidney Disease and Cardiac Hypertrophy

Kohei Okamoto,[1] **Hideki Fujii,**[1] **Kentaro Watanabe,**[1] **Shunsuke Goto,**[1] **Keiji Kono,**[1] **and Shinichi Nishi**[1]

[1]Division of Nephrology and Kidney Center, Kobe University Graduate School of Medicine, Kobe, Hyogo 650-0017, Japan

Correspondence: Hideki Fujii, MD, PhD, Division of Nephrology and Kidney Center, Kobe University Graduate School of Medicine, 7-5-2, Kusunoki-cho, Chuo-ku, Kobe, Hyogo 650-0017, Japan. Email: fhideki@med.kobe-u.ac.jp.

Abstract

Serum fibroblast growth factor 23 (FGF23) levels and the renin-angiotensin-aldosterone system (RAAS) are elevated in chronic kidney disease (CKD) patients, and their association with left ventricular hypertrophy (LVH) has been reported. However, whether the FGF23 elevation is the cause or result of LVH remains unclear. At 10 weeks, male C57BL/6J mice were divided into 4 groups: sham, CKD (5/6 nephrectomy), LVH (transaortic constriction), and CKD/LVH group. At 16 weeks, the mice were euthanized, and blood and urine, cardiac expressions of FGF23 and RAAS-related factors, and cardiac histological analyses were performed. Heart weight, serum FGF23 levels, and cardiac expression of FGF23 and RAAS-related factors, except for angiotensin-converting enzyme 2, were more increased in the CKD/LVH group compared to the other groups. A significant correlation between LVH and cardiac expressions of FGF23 and RAAS-related factors was observed. Furthermore, there was a significantly close correlation of the cardiac expression of FGF23 with LVH and RAAS-related factors. The coexisting CKD and LVH increased serum and cardiac FGF23 and RAAS-related factors, and there was a significant correlation between them. A close correlation of cardiac, but not serum FGF23, with LVH and RAAS suggests that local FGF23 levels may be associated with LVH and RAAS activation.

Key Words: aldosterone, chronic kidney disease, fibroblast growth factor 23, left ventricular hypertrophy, renin-angiotensin-aldosterone system

Abbreviations: 25(OH)D, 25-hydroxyvitamin D; 1,25(OH)$_2$D, 1, 25-dihydroxyvitamin D; α-MHC, α-myosin heavy chain; β-MHC, β-myosin heavy chain; ACE, angiotensin-converting enzyme; AGT, angiotensinogen; ANP, atrial natriuretic peptide; AT1R, angiotensin II type 1 receptor; BNP, brain natriuretic peptide; BP, blood pressure; CKD, chronic kidney disease; CKD-MBD, chronic kidney disease and mineral bone disorder; Col1a2, collagen type I α2; Col3a1, collagen type III α2; FGF23, fibroblast growth factor 23; FGFR, fibroblast growth factor 23 receptor; GAPDH, glyceraldehyde 3-phosphate dehydrogenase; iFGF23, intact fibroblast growth factor 23; iPTH, intact parathyroid hormone; LVH, left ventricular hypertrophy; MAPK, mitogen-activated protein kinase; mRNA, messenger RNA; NFAT, nuclear factor of activated T cells; qPCR, quantitative polymerase chain reaction; RAAS, renin-angiotensin-aldosterone system; TAC, transverse aortic constriction; u8-OHdG, urinary 8-hydroxy-2′-deoxyguanosine; uAGT, urinary angiotensinogen; uAlb, urinary albumin.

Fibroblast growth factor 23 (FGF23) is a crucial phosphaturic hormone, and its serum level increases as kidney function declines [1]. FGF23 is mainly produced in bones and interacts with the FGF23 receptor (FGFR) in the presence of Klotho in the kidney proximal tubules. In this way, phosphorus diuresis is promoted in the kidney. However, FGF23 also has many other functions [2]. One of them is potential paracrine action on the progression of left ventricular hypertrophy (LVH) [3-5]. Although previous experimental studies have reported that considerably high levels of serum FGF23 could induce LVH via FGFR4-mediated calcineurin–nuclear factor of activated T cells (NFAT) pathway activation even in the absence of αKlotho [4], clinical studies have shown a significant correlation between serum FGF23 levels and LVH even in patients with a mild or moderate elevation of serum FGF23 levels [3]. In addition, it has also been reported that the *FGF23* gene–deletion mice underwent transverse aortic constriction (TAC) present with LVH [6]. Although patients with tumor-induced osteomalacia have remarkably high serum FGF23 levels and FGF23-related hypophosphatemia, serum FGF23 levels are not

associated with LVH [7]. Thus, it is unclear whether LVH progresses owing to an increase in FGF23 levels or whether the occurrence of LVH causes FGF23 levels to increase, and, currently, there is no consensus on which is the primary cause [8].

Recent studies have demonstrated a close correlation between FGF23 and the renin-angiotensin-aldosterone system (RAAS) [9]. The RAAS is an important system for controlling blood pressure (BP) and causes LVH [10]. Therefore, we focused on the RAAS as the common factor influencing the increase in FGF23 levels and the exacerbation of LVH.

This study aimed to investigate alterations in FGF23 and RAAS and their correlation using a chronic kidney disease (CKD) model, a pressure overload-induced cardiac hypertrophy model, and a combined model.

Material and Methods

Animals

Male C57BL/6J mice were obtained from SLC Japan Inc. The mice were housed with ad libitum food and water

under light- and temperature-controlled environments. The mice were randomly divided into 4 groups at age 10 weeks: sham-operated mice (sham, n = 6), induced-CKD mice (CKD, n = 6), induced-LVH mice (LVH, n = 6), and induced-CKD and induced-LVH mice (CKD/LVH, n = 6). At age 10 weeks, TAC was performed in the mice in the LVH and CKD/LVH groups. Briefly, the mice were anesthetized using isoflurane, followed by intraperitoneal administration of medetomidine, midazolam, and butorphanol. They were subsequently intubated with 22-G vascular catheters and then artificially ventilated (Small Animal Ventilator MK-V100, Muromachi Kikai). The thorax was opened, the aorta was exteriorized and a ligature was placed around the aorta as described previously [11]. The needle used for ligation was a 27-G needle. At age 11 weeks, a left two-thirds nephrectomy was performed, and 1 week later, a right nephrectomy was performed in the mice in the CKD and CKD/LVH groups. For mice in the sham group, sham operations were performed at age 10, 11, and 12 weeks. The echocardiographic parameters were measured and the 24-hour urine samples were collected from each mouse using a metabolic cage before euthanizing them at age 16 weeks under anesthesia. The blood samples for serum measurements were collected from the right ventricle, and the hearts and bones were removed for RNA extraction and histomorphological analysis.

This study was carried out in strict accordance with the recommendations outlined in the Guide for the Care and Use of Laboratory Animals of the National Institutes of Health. The protocol was approved by the Animal Experiment Facility Ethics Committee, Graduate School of Medicine, Kobe University (Permit No.: P160707-R2). All surgical procedures were performed under anesthesia using 1.5% isoflurane with intraperitoneally administered medetomidine (0.15 mg/kg), midazolam (2 mg/kg), and butorphanol (2.5 mg/kg) premedications. Efforts were made to minimize animal suffering by following the ARRIVE guidelines for reporting experiments involving animals [12, 13]. A randomized protocol was adopted for the experiments on 24 mice.

Blood and Urine Measurements

The collected blood samples were centrifuged for 15 minutes at 3000 rpm and stored at –80 °C until analysis. Serum creatinine (Cr) levels were measured using Fuji Dri-chem 3500 (FUJIFILM Japan). Serum phosphate levels were measured using a Phospha-C test Wako (FUJIFILM Japan). Urinary Cr levels were measured using LabAssay Cr (FUJIFILM Wako Pure Chemicals Corp). Serum intact parathyroid hormone (iPTH), intact fibroblast growth factor 23 (iFGF23), and aldosterone levels were measured using an enzyme-linked immunosorbent assay (iPTH: CEA866Mu, Cloud-Clone Corp, RRID: AB_2895005; iFGF23: CY-4000, Kainos Laboratories Inc, RRID: AB_2782966; aldosterone: ab136933, Abcam, RRID: AB_2895004). Further, urinary albumin (uAlb) levels, urinary angiotensinogen (uAGT) levels, and urinary 8-hydroxy-2′-deoxyguanosine (u8-OHdG) were also determined using an enzyme-linked immunosorbent assay (uAlb: AKRAL-121, FUJIFILM Wako Shibayagi Corp, RRID: AB_2895006; uAGT: MBS760284, MyBioSource, RRID: AB_2895007; u8-OHdG: KOG-200SE, Japan Institute for the Control of Aging, RRID: AB_2895008). Serum 25-hydroxyvitamin D (25D) and 1, 25-dihydroxyvitamin D (1,25D) levels were measured using the 25D125I radioimmunoassay kit (KIP1971, DIAsource

ImmunoAssays SA, RRID: AB_2895009) and the TFB 1,25D radioimmunoassay kit (AA-54F1, Immunodiagnostic Systems Ltd, RRID: AB_2895011), respectively.

Blood Pressure Measurements

BP was measured using tail-cuff plethysmography (Model MK-2000; Muromachi Kikai Co Ltd). The mice were rested for 15 minutes to reduce stress-induced BP elevation. The mean BP values were finally determined from multiple readings (at least 10). BP evaluation was performed at the end of the study period.

Echocardiographic Measurements

The mice were mildly anesthetized using 1.0% isoflurane. Echocardiography was performed using a commercially available echocardiographic system (F37; Hitachi Aloka Medical Ltd). The wall thickness and ejection fraction were measured using a 2-dimensional short-axis view of the LV at the papillary muscle level. These studies were performed on mice aged 16 weeks.

Histological and Immunohistochemical Analyses

The hearts of the mice were removed, weighed, and fixed in 10% formaldehyde. The paraffin block was then prepared by immersing the samples in ethanol, xylene, and paraffin in the embedding device at room temperature. The paraffin blocks were cut into 2-μm-thick sections and stained with hematoxylin-eosin for routine histology and Sirius red for further morphometric studies.

FGF23, angiotensin II, angiotensin-converting enzyme (ACE), and ACE2 expressions in the hearts were assessed using anti-FGF23 monoclonal antibodies (R&D Systems), antiangiotensin II monoclonal antibodies (Novus Biologicals LLC), anti-ACE monoclonal antibodies (Abcam), and anti-ACE2 monoclonal antibodies (R&D Systems), respectively. Briefly, the heart slices were preincubated with blocking agents and subsequently incubated with the aforementioned primary antibodies for 60 minutes at room temperature (ACE, FGF23) and then overnight at 4 °C (ACE2, angiotensin II). Biotinylated antirat and antigoat immunoglobulin G (Vector Laboratories Inc) and an avidin:biotinylated enzyme complex (VECTASTAIN Elite ABC Reagent; Vector Laboratories Inc) for FGF23 and ACE2 and a universal immunoperoxidase polymer (Histofine Simple Stain mouse MAX PO, antirat and antirabbit; Nichirei) for ACE and angiotensin II were used for immunostaining.

The means of percentage of positive areas observed using Sirius red staining, relative immune-positive area, and cardiomyocyte width and area in the left ventricular (LV) sections were calculated from 20 randomly selected microscopic fields using ImageJ software (Image J, US National Institutes of Health). As for assessing the immune-positive area, the relative value was defined as that in each group compared to that in the sham group. All evaluations were performed in a blinded manner.

RNA Extraction and Real-Time Polymerase Chain Reaction

As previously reported [14, 15], total RNA was extracted from the mouse heart and bone samples with an ISOGEN kit (Wako Pure Chemicals Industries Ltd) according to the manufacturer's instructions. The ReverTra Ace quantitative

polymerase chain reaction (qPCR) RT Kit (TOYOBO Co Ltd) was used to create complementary DNA using an oligo-dT primer as recommended by the manufacturer. The synthesized complementary DNA was stored at −80 °C until analysis via qPCR. The messenger RNA (mRNA) expression was examined via real-time PCR using the Applied Biosystems 7500 Real-Time PCR System (Thermo Fisher Scientific) along with the SYBR Green Assay with the Thunderbird SYBR qPCR Mix (TOYOBO Co Ltd) following the manufacturers' protocol. The analysis was performed using the relative quantification method of the Applied Biosystems 7500 Real-Time PCR Software. The relative mRNA expressions in the samples were normalized to glyceraldehyde 3-phosphate dehydrogenase (GAPDH) mRNA expression. For PCR analysis, we used the following primers: α-myosin heavy chain (α-MHC; 5′-ATGTTAAGGCCAAGGTCGTG-3′, 5′-CAC CTGGTCCTCCTTTATGG-3′), β-myosin heavy chain (β-MHC; 5′-AGCATTCTCCTGCTGTTTCC-3′, 5′-GAGCCT TGGATTCTCAAACG-3′), atrial natriuretic peptide (ANP; 5′-AGGCAGTCGATTCTGCTTGA-3′, 5′-CGTGATAGA TGAAGGCAGGAAG-3′), brain natriuretic peptide (BNP; 5′-TAGCCAGTCTCCAGAGCAATTC-3′, 5′-TTGGTCCT TCAAGAGCTGTCTC-3′), Collagen type I α2 (Col1a2; 5′-GCAGGTTCACCTACTCTGTCCT-3′, 5′-CTTGCCCCA TTCATTTGTCT-3′), Col3a1 (5′-TCCCCTGGAATCTGTG AATC-3′, 5′-TGAGTCGAATTGGGGAGAAT-3′), connective tissue growth factor (CTGF) (5′-CACAGAGTGGAGCGC CTGTTC-3′, 5′-GATGCACTTTTTGCCCTTCTTAA-3′), FGF23 (5′-ACAAGGACACCTAAACCGAACAC-3′, 5′-AGC TACTGACTGGTCCTATCACA-3′), angiotensinogen (AGT; 5′-TCTCTTTACCCCTGCCCTCT-3′, 5′-GAAA CCTCTCATCGTTCCTTG-3′), angiotensin II type 1 receptor (AT1R; 5′-CCATTGTCCACCCGATGAAG-3′, 5′-TGCAGGTGACTTTGGCCAC-3′), ACE (5′-CCCTAGA GAAAATCGCCTTCTTG-3′, 5′-CGAAGATACCACCAGT CGAAGTT-3′), ACE2 (5`-TGGGCAAACTCTATGCTG-3′, 5′-TTCATTGGCTCCGTTTCTTA-3′), renin (5′-CCTCT ACCTTGCTTGTGGGATT-3′, 5′-CTGGCTGAGGGAAAC CTTTGACT-3′), and GAPDH (3′-GCAAAGTGGAGATT GTTGCCA-5′, 3′-AATTTGCCGTGAGTGGAGTCA-5′).

Statistical Analyses

The collected data were analyzed using IBM SPSS software (version 25.0; IBM Corp) for all statistical analyses. Values are presented as means ± SEM. The Mann-Whitney *U* test was used to analyze the significance of differences between the 2 groups. The Kruskal-Wallis test was used to assess the differences among the 4 groups. Pearson and Spearman correlation coefficients were used to analyze the relationships between the variables. A *P* value of less than .05 was considered to indicate statistical significance.

Results

Animal Characteristics and Biochemical Measurements

The characteristics and biochemical data of the mice at age 16 weeks in the sham, CKD, LVH, and CKD/LVH groups are shown in Table 1. Systolic BP was statistically significantly elevated in the CKD and CKD/LVH groups. Serum Cr levels, phosphate levels, and uAlb excretion in the CKD and CKD/LVH groups were statistically significantly increased

compared to those in the sham group. Serum calcium levels were comparable among the 4 groups. Although uAlb excretion was comparable between the sham and LVH groups, serum Cr levels in the LVH group were slightly elevated compared to those in the sham group. Serum iPTH levels in the CKD and LVH groups were elevated compared to those in the sham group, albeit not statistically significantly; however, they were statistically significantly higher in the CKD/LVH group. Serum 25D levels were similar among all the study groups, and serum 1,25D levels were decreased by CKD induction. Urinary 8-OHdG levels were statistically significantly higher in the CKD and CKD/LVH groups than in the sham group. As shown in Fig. 1, although serum iFGF23 levels were statistically significantly elevated in the CKD, LVH, and CKD/LVH groups relative to those in the sham group, no statistically significant difference was noted among the 3 groups, except for that in the sham group. In contrast, serum aldosterone levels increased by CKD and LVH induction, and they were additionally increased by coexisting CKD and LVH.

Cardiac Parameters After Chronic Kidney Disease and Left Ventricular Hypertrophy Induction

Cardiac parameters evaluated using echocardiography and heart weight are shown in Table 2. As for LV dimension, LV end-diastolic diameter and LV end-systolic diameter in the CKD/LVH group were smaller compared to those in the other groups. Both anterior and posterior walls of the LV were remarkably thickened in the LVH and CKD/LVH groups. Systolic function evaluated as ejection fraction was statistically significantly reduced in the LVH and CKD/LVH groups compared with the sham and CKD groups. The relative heart weight (heart weight/body weight) was significantly higher in the order of the CKD/LVH, LVH, CKD, and sham groups.

Coexisting Chronic Kidney Disease and Left Ventricular Hypertrophy Cause Cardiac Hypertrophy and Cardiac Interstitial Fibrosis to Deteriorate

As shown in Fig. 2, cardiomyocyte width and area increased by LVH and CKD induction. Coexisting LVH and CKD are related to the further development of cardiac hypertrophy. Cardiac fibrosis was also statistically significantly exacerbated in the CKD/LVH groups (Fig. 3).

Cardiac Expressions of Fibroblast Growth Factor 23, Renin-Angiotensin-Aldosterone System–related Factors, and Cardiac Hypertrophy–related Factors Induced by Chronic Kidney Disease and Left Ventricular Hypertrophy

Cardiac FGF23 mRNA expression was statistically significantly increased in the LVH group and further increased in the CKD/LVH group. Similarly, cardiac angiotensinogen (Ang) mRNA expression was statistically significantly increased in the LVH group and further increased in the CKD/LVH group. Cardiac AT1R and angiotensin-converting enzyme (ACE) mRNA expressions were statistically significantly increased in the CKD/LVH group. In contrast, cardiac ACE2 mRNA expression was statistically significantly decreased in the LVH group and further decreased in the CKD/LVH group (Fig. 4).

Immunohistochemical analysis revealed that FGF23 and ACE expressions were statistically significantly increased in the CKD/LVH group. Corresponding with real-time PCR

Table 1. Animal characteristics at 16 weeks

	Sham	CKD	LVH	CKD/LVH
	(N = 6)	(N = 6)	(N = 6)	(N = 6)
Body weight, g	29. 5 ± 0.7	25.1 ± 0.8[a]	28.7 ± 0.6[b]	25.7 ± 1.0[a,c]
SBP, mm Hg	86.2 ± 0.6	97.6 ± 2.0[a]	87.2 ± 1.8	107.2 ± 4.0[a,c]
HR, /min	516.3 ± 12.3	493.1 ± 12.2	490.7 ± 15.4	472.8 ± 14.7
Cr, mg/dL	0.14 ± 0.02	0.44 ± 0.03[a]	0.23 ± 0.02[b]	0.47 ± 0.09[a,c]
Ca, mg/dL	9.87 ± 0.30	9.83 ± 0.80	10.03 ± 0.76	9.02 ± 0.81
P, mg/dL	8.1 ± 0.6	9.7 ± 0.4[a]	8.8 ± 0.3	10.3 ± 0.3[a]
iPTH, pg/mL	29.0 ± 11.6	77.6 ± 16.2	50.6 ± 7.0	111.6 ± 39.1[a]
25(OH)D, pg/mL	61.7 ± 2.3	61.8 ± 3.5	59.7 ± 3.2	63.3 ± 4.0
1, 25(OH)$_2$D, pg/mL	227.0 ± 18.9	184.8 ± 10.4	222.2 ± 24.6	178.0 ± 9.9
uAGT, ng/mgCr	3.32 ± 0.85	3.36 ± 0.94	7.13 ± 2.55[a,b]	9.62 ± 2.10[a,b]
uAlb, μg/mgCr	144.6 ± 9.5	1156.3 ± 221.2[a]	156.1 ± 5.7[b]	1356.8 ± 145.6[a,c]
u8-OHdG, ng/mgCr	53.9 ± 1.8	99.4 ± 16.1[a]	82.8 ± 8.3	101.3 ± 9.2[a]

Abbreviations: 1,25(OH)$_2$D, 1,25-dihydroxyvitamin D; 25(OH)D, 25-hydroxyvitamin D; Ca, calcium; CKD, chronic kidney disease; Cr, creatinine; HR, heart rate; iPTH, intact parathyroid hormone; LVH, left ventricular hypertrophy; P, phosphate; SBP, systolic blood pressure; u8-OHdG, urinary 8-hydroxy-2′-deoxyguanosine; uAGT, urinary angiotensinogen; uAlb, urinary albumin.
[a]vs sham, *P* less than .05.
[b]vs CKD, *P* less than .05.
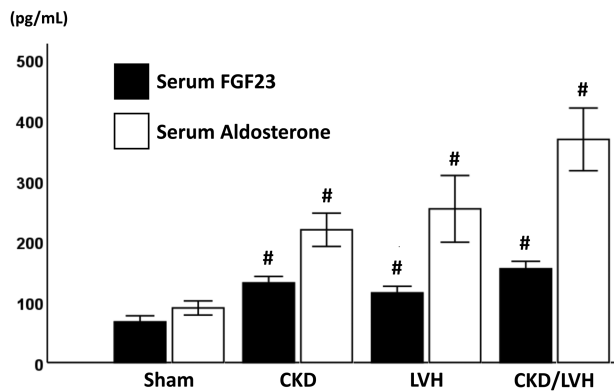[c]vs LVH, *P* less than .05.

Figure 1. Serum fibroblast growth factor 23 (FGF23) and aldosterone levels among the study groups. Black bar: serum FGF23 levels. White bar: serum aldosterone levels. #vs sham group, *P* less than .05.

results, angiotensin II was statistically significantly increased in the LVH and CKD/LVH groups, and the ACE2 expression was statistically significantly decreased in the LVH and CKD/LVH groups (Fig. 5).

FGF23 mRNA expression in bones was slightly increased in the LVH group than in the sham group and remarkably increased by CKD induction (Fig. 6).

Messenger RNA Expression of Factors Related to Cardiac Hypertrophy and Fibrosis Increased by Chronic Kidney Disease and Left Ventricular Hypertrophy Induction

The mRNA expressions of β-MHC, ANP, BNP, Col1a2, and Col3a1 in cardiac tissues were statistically significantly increased, whereas those of α-MHC were decreased in the CKD/LVH group. In the LVH group, cardiac β-MHC mRNA expression was statistically significantly increased, and α-MHC mRNA expression was statistically significantly decreased in cardiac tissues of mice in

the LVH group compared with those of mice in the sham group (Fig. 7).

Correlation of Fibroblast Growth Factor 23 and Renin-Angiotensin-Aldosterone System–related Factors With Cardiac Hypertrophy and Fibrosis

Serum FGF23 levels, cardiac FGF23 expression (mRNA and immunohistochemical staining), and RAAS-related factors were related to cardiac hypertrophy parameters (width and size of cardiomyocyte) and mRNA expressions of factors related to cardiac hypertrophy and fibrosis. However, the correlation of serum FGF23 levels with them was weaker than that of cardiac FGF23 expression and RAAS-related factors (Table 3). Although cardiac FGF23 expression was statistically significantly correlated with all RAAS-related factors, serum FGF23 levels were statistically significantly correlated with only cardiac AT1R and AGT mRNA expressions and angiotensin II and ACE immunohistochemical expressions (Table 4). Thus, the correlation of cardiac FGF23 expression with RAAS-related factors was closer than that of serum FGF23 levels with RAAS-related factors.

Discussion

We demonstrated that 1) CKD exacerbated LVH and cardiac fibrosis induced by TAC; 2) serum FG23 and aldosterone levels were increased in the CKD and LVH groups, which were further elevated in the CKD/LVH group; 3) similarly, intracardiac FGF23, hypertrophy-related factors, fibrosis-related factors, and RAAS-related factors were increased in the LVH and CKD groups and dramatically increased in the CKD/LVH group; 4) among the RAAS-related factors, only ACE2 was decreased by LVH, CKD, and CKD/LVH induction; and 5) heart weight was statistically significantly correlated with serum FGF23 and aldosterone levels and intracardiac FGF23 and RAAS-related factor expressions.

Table 2. Animal characteristics at 16 weeks

	Sham	CKD	LVH	CKD/LVH
	(N = 6)	(N = 6)	(N = 6)	(N = 6)
LVDd, mm	3.77 ± 0.76	3.45 ± 0.76	3.47 ± 0.29	3.15 ± 0.08
LVDs, mm	2.78 ± 0.06	2.67 ± 0.06	2.75 ± 0.22	2.55 ± 0.07[a,b]
LVAW, mm	0.75 ± 0.02	0.80 ± 0.04	1.23 ± 0.04[a,b]	1.30 ± 0.04[a,b]
LVPW, mm	0.71 ± 0.03	0.75 ± 0.04	1.18 ± 0.05[a,b]	1.20 ± 0.04[a,b]
FS, %	25.8 ± 0.4	23.0 ± 0.2[a]	20.9 ± 0.3[a,b]	19.3 ± 0.8[a,b]
EF, %	57.7 ± 0.6	52.9 ± 0.4	49.1 ± 0.5[a,b]	46.0 ± 1.7[a,b]
Heart weight, mg	131.3 ± 3.3	116.2 ± 2.3	181.6 ± 5.2[a,b]	178.2 ± 8.5[a,b]
Relative heart weight, mg/g	4.45 ± 0.07	4.64 ± 0.08	6.33 ± 0.16[a,b]	6.96 ± 0.36[a,b]

Abbreviations: CKD, chronic kidney disease; EF, ejection fraction; FS, fractional shortening; LVAW, left ventricular anterior wall; LVDd, left ventricular diastolic diameter; LVDs, left ventricular systolic diameter; LVH, left ventricular hypertrophy; LVPW, left ventricular posterior wall.
[a]vs sham, *P* less than .05.
[b]vs CKD, *P* less than .05.
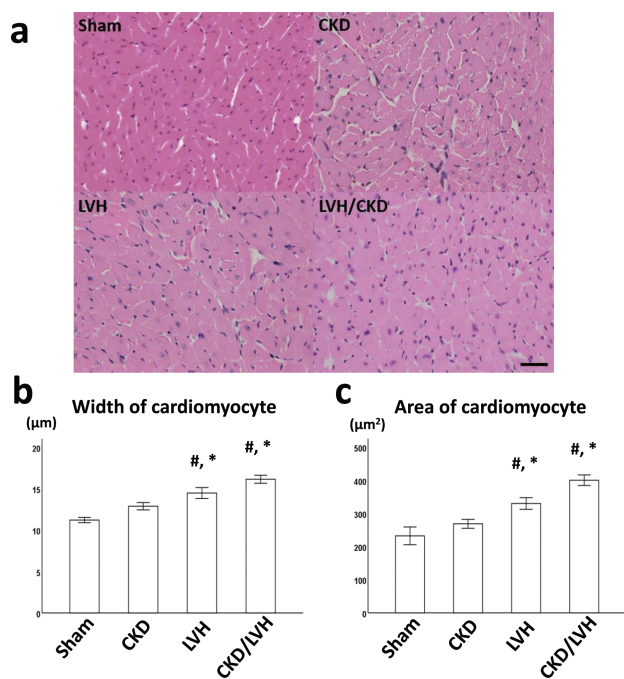[c]vs LVH, *P* less than .05.

Figure 2. Histological analysis of cardiomyocytes. Representative photomicrographs of cardiomyocytes stained with hematoxylin-eosin (magnification, ×400; scale bar = 50 μm). Upper left panel, sham group; upper right panel, chronic kidney disease (CKD) group; lower left panel, left ventricular hypertrophy (LVH) group; lower right panel, CKD/LVH group. A, Width of cardiomyocytes. B, Area of cardiomyocytes. Values are expressed as means ± SEM. #vs sham, *P* less than .05; *vs CKD, *P* less than .05.

It is well known that pressure overload and CKD induce LVH. The development of LVH in these conditions involves various pathophysiological mechanisms. In pressure overload–induced LVH, cardiomyocyte hypertrophy and interstitial fibrosis reportedly occur owing to the activation of mitogen-activated protein kinase (MAPK) pathway [16], increase in oxidative stress [17], and activation of RAAS [18]. The results of our study also demonstrated increased urinary excretion of 8-OHdG, elevated serum aldosterone levels, and increased cardiac expression of AT1R, AGT, and ACE.

In CKD, not only these factors but also CKD-related factors are involved in LVH progression. Recent compelling evidence suggests that CKD and mineral bone disorder (CKD-MBD) is strongly linked to the progression of cardiovascular disease in these populations [19]. Among the CKD-related factors, phosphate, calcium, FGF23, PTH, Klotho, and 1,25 $(OH)_2D$ are thought to play key roles [20, 21]. Many experimental and clinical studies have reported a correlation between FGF23 and LVH [3, 22]. Further, elevated FGF23 levels directly result in myocardial hypertrophy even if Klotho does not co-exist with FGFR [4, 23]. Among FGFRs, FGFR4 is thought to have an important role in LVH progression through the activation of the calcineurin-NFAT pathway [4, 24]. However, a previous experimental study using cardiomyocyte-specific calcineurin A–transgenic mice showed that LVH induced an increase in myocardial and serum FGF23 levels [24]. In other words, this might mean that the activation of the calcineurin-NFAT pathway could increase FGF23 levels. Therefore, we performed an experimental study using surgical models of CKD, LVH, and CKD/LVH to ascertain alterations in RAAS and CKD-MBD parameters, including FGF23. Although serum and cardiac FGF23 levels increased in CKD as previously reported, they also increased in LVH without CKD. Further elevation of FGF23 levels were observed in CKD/LVH. However, as serum FGF23 levels in the CKD/LVH group were approximately 2-fold higher compared to those in the sham group, they did not seem to be enough to bind to FGFR without Klotho.

On the other hand, serum aldosterone levels in the CKD group were approximately 5-fold higher than those in the sham group, and intracardiac mRNA expression of RAAS-related factors was also increased in the CKD/LVH group. In our previous study using hypertensive model rats, an increase in serum FGF23 levels was also trivial [25]. In contrast, the increase in serum aldosterone levels was much greater in the hypertensive group than in the sham group. Furthermore, serum FGF23 levels were not correlated with LVH in pediatric CKD patients with preserved kidney function and FGF23-related hypophosphatemic diseases [7, 26]. From these findings, it is speculated that the influence of RAAS on LVH is greater than that of FGF23.

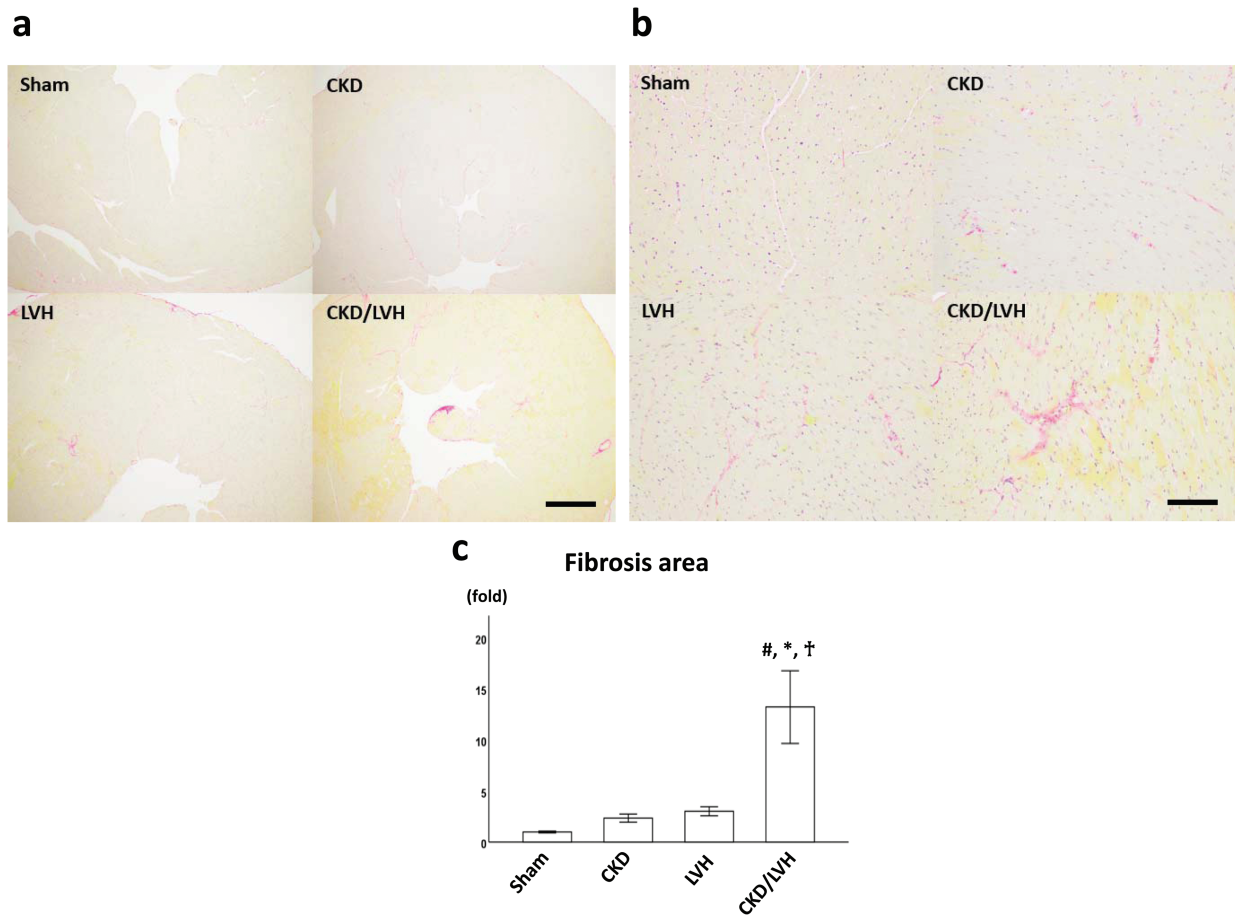To date, various studies have reported the interaction between RAAS and FGF23 [27-30]. An in vitro study using

Figure 3. Evaluation of cardiac fibrosis. A, Representative photomicrographs of cardiomyocytes with Sirius red (magnification, ×40; scale bar = 500 µm). Upper left panel, sham group; upper right panel, chronic kidney disease (CKD) group; lower left panel, left ventricular hypertrophy (LVH) group; lower right panel, CKD/LVH group. B, Representative photomicrographs of cardiomyocytes stained with Sirius red (magnification, ×200; scale bar = 100 µm). Upper left panel, sham group; upper right panel, CKD group; lower left panel, LVH group; lower right panel, CKD/LVH group. C, Fibrosis area in the heart. Values are expressed as means ± SEM. #vs sham, *P* less than .05; *vs CKD, *P* less than .05; †vs LVH, *P* less than .05.
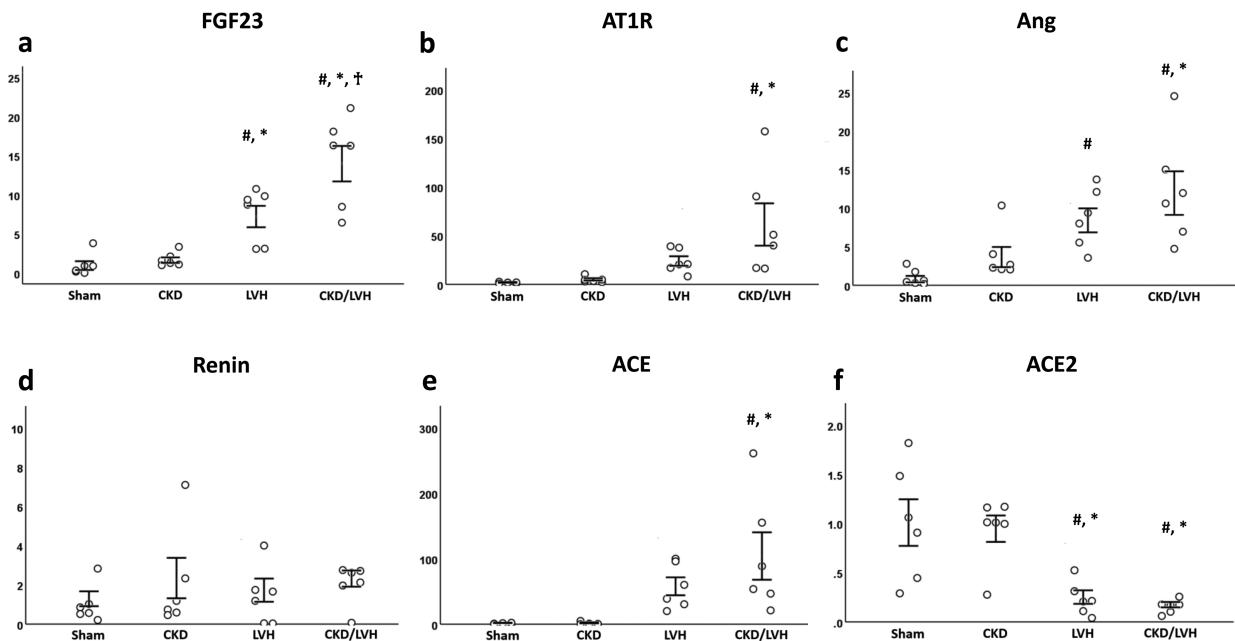

Figure 4. Messenger RNA expressions of fibroblast growth factor 23 (FGF23) and renin-angiotensin-aldosterone system (RAAS)-related factors in the heart. A, FGF23. B, Angiotensin II type 1 receptor (AT1R). C, Angiotensinogen (Ang). D, Renin. E, Angiotensin-converting enzyme (ACE). F, Angiotensin-converting enzyme 2 (ACE2). Values are expressed as means ± SEM. #vs sham, *P* less than .05; *vs chronic kidney disease (CKD), *P* less than .05; †vs left ventricular hypertrophy (LVH), *P* less than .05.
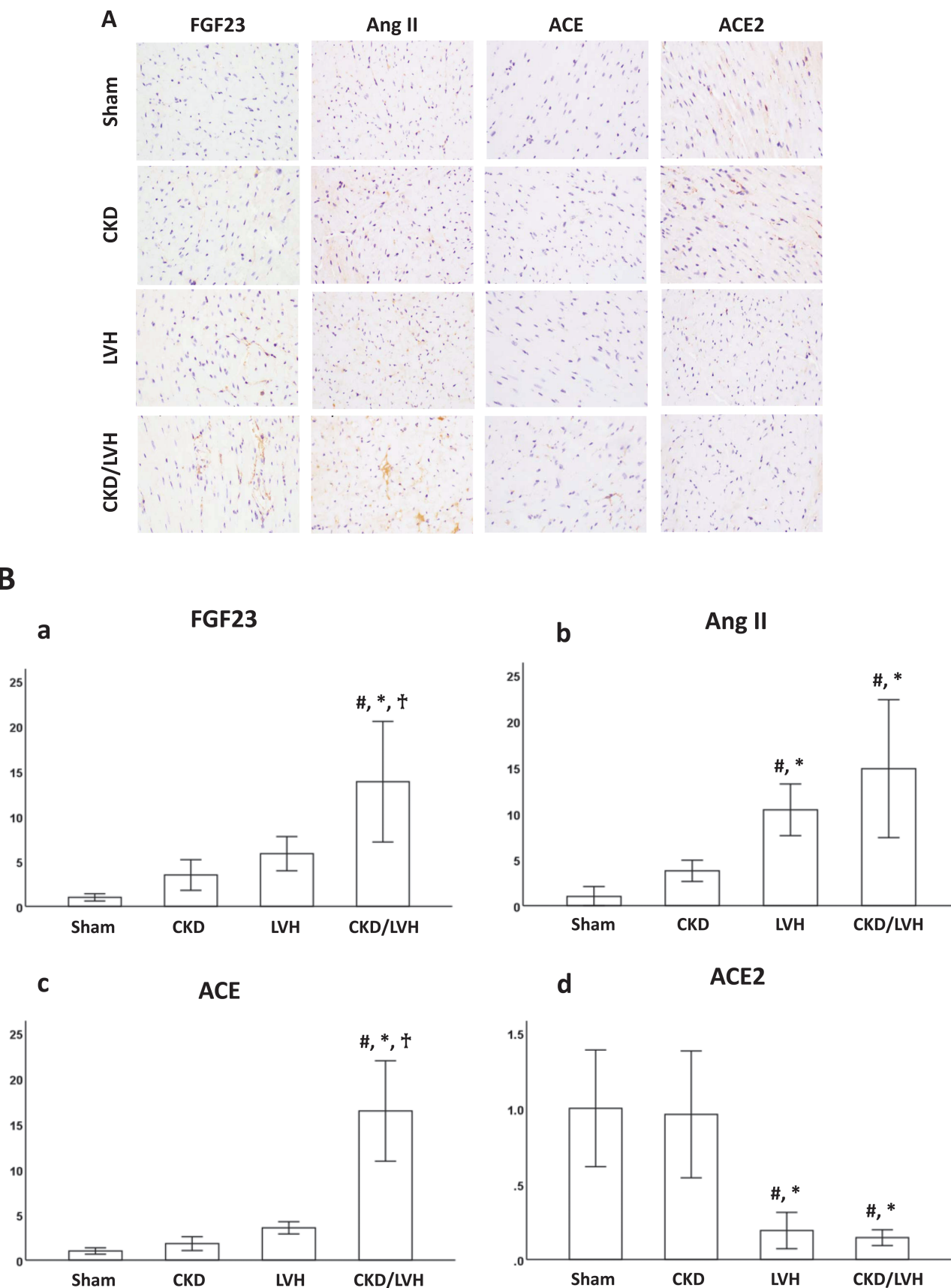
Figure 5. Evaluation of the expressions of fibroblast growth factor 23 (FGF23) and renin-angiotensin-aldosterone system (RAAS)-related factors via immunohistochemical staining. A, Representative photomicrographs of cardiomyocytes with immunohistochemical staining for FGF23 and RAAS-related factors (magnification, ×400; scale bar = 50 µm). B, Semiquantitative evaluation of FGF23 and RAAS-related factors in the heart. a, FGF23. b, Angiotensin II (Ang II). c, Angiotensin-converting enzyme (ACE). d, Angiotensin-converting enzyme 2 (ACE2). Values are expressed as means ± SEM. #vs sham, *P* less than .05; *vs chronic kidney disease (CKD), *P* less than .05; †vs left ventricular hypertrophy (LVH), *P* less than .05.
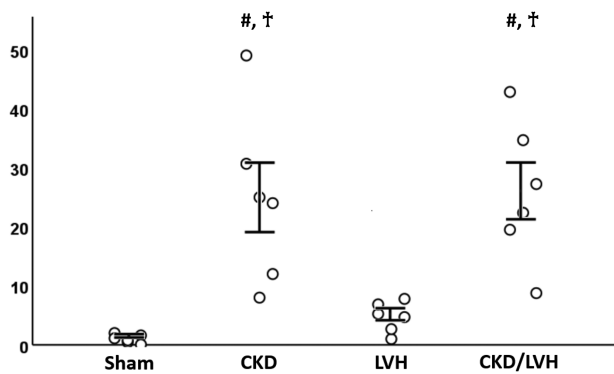
Figure 6. Messenger RNA expression of fibroblast growth factor 23 (FGF23) in bones. Values are expressed as means ± SEM. #vs sham, *P* less than .05; †vs left ventricular hypertrophy (LVH), *P* less than .05.

cardiomyocytes demonstrated that angiotensin II and aldosterone significantly upregulated FGF23 mRNA expression, suggesting that RAAS activation leads to FGF23 upregulation in cardiomyocytes [31]. In contrast, FGF23 also increased intracellular angiotensin II expression in cardiomyocytes [9]. RAAS and FGF23 are both thought to be closely related to the pathophysiological mechanisms underlying the progression of LVH and cardiac fibrosis. Our previous study showed a statistically significant relationship between serum FGF23 and aldosterone levels, in which both were statistically significantly correlated with heart weight [25]. Similarly, in the present study, RAAS-related factors and FGF23 were both increased in cardiac tissues in the CKD and LVH groups. This increase was particularly evident in the CKD/LVH group. Serum FGF23 levels, intracardiac FGF23 expression, serum aldosterone levels, and intracardiac RAAS-related factors expressions were statistically significantly correlated with heart weight. Particularly, a statistically significantly close correlation between intracardiac RAAS-related factors and FGF23 was observed. There surely is a close link between intracardiac RAAS and FGF23, which possibly plays a key role in LVH progression. Certainly, we could not exclude the effect of serum FGF23 in this study. However, the correlation of local FGF23 and RAAS expressions with LVH was stronger than that of serum FGF23 levels with LVH. Considering the results of the present study and other studies [6-8], we also wonder whether mild elevation of serum FGF23 levels could affect LVH. This issue remains to be resolved.

We also assessed the influence of LVH on CKD-MBD parameters. An increase in FGF23 decreases 1,25 $(OH)_2D$ via reduced expression of 1α-hydroxylase [32] and leads to increased renin activity [33]. In addition, $1,25(OH)_2D$ is also considered a crucial factor in LVH progression because cardiac-specific vitamin D receptor knockout mice reportedly show marked cardiac hypertrophy [34]. Further, a vitamin D receptor activator can prevent LVH progression independently of RAAS [35]. The present study also showed that serum $1,25(OH)_2D$ decreased in the CKD and CKD/LVH groups despite similar serum 25(OH)D levels. ACE2 is an enzyme that can convert angiotensin I to angiotensin (1-9) and angiotensin II to angiotensin (1-7) [36, 37]. Angiotensin (1-9) and angiotensin (1-7) can lower

BP by their vasodilative effects. Thus, they can prevent LVH progression. ACE2-deficient mice demonstrate cardiac dysfunction and LVH, increased oxidative stress, and inflammatory cytokine expression [38-40]. Interestingly, intracardiac ACE2 expression dramatically decreased in the LVH and CKD/LVH groups, and ACE is supposed to be an important factor in the progression of LVH. It has been reported that FGF23 decreases ACE2 expression [41] and that plasma ACE2 activity is impaired in patients with CKD [42]. Therefore, this mechanism might greatly contribute to the progression of LVH in CKD.

This study had several limitations. The most important limitation of this study is that we could not clarify the first occurrence regarding the relationship between RAAS and FGF23. So far, no studies have examined which of FGF23 and RAAS increases the first. The reason is because it is difficult to eliminate the influence of other factors because of the complex interaction. Second, the activation of RAAS in CKD does not necessarily occur in all forms of renal failure. Although the pathophysiology of hyporeninemic hypoaldosteronism resulting from decreased renin secretion due to sclerosis of the juxtaglomerular apparatus has been also reported [43], many CKD patients are considered under the condition of activated RAAS, and it contributes to the progression of kidney dysfunction [14, 44]. Therefore, we consider that this relationship may be important in most CKD patients. Third, from the degree of change in FGF23, we supposed that FGF23 could not be a contributor to the progression of LVH. However, there is a possibility that FGF23 may induce LVH in a paracrine or autocrine manner, or both. FGF23 and RAAS enhance the expression of cardiac hypertrophy- and cardiac fibrosis–related factors via various pathways, such as the MAPK, transforming growth factor-β (TGF-β)–Smad, nuclear factor κB, and NFAT-CnB pathways [15, 16, 24]. Unfortunately, our study could not adequately evaluate these pathways. As for intracardiac calcineurin B expression, there was no statistically significant difference among the study groups. Fourth, we did not perform an interventional study with any FGFR blocker, ACE inhibitor, angiotensin receptor blocker, or aldosterone blocker. A previous study demonstrated that FGFR4-null mice did not develop LVH in response to elevated FGF23 expression, and the overexpression of FGFR4 induced LVH even in non-CKD mice [23]. Therefore, we believe that FGF23 may not be a mere biomarker. Although we speculated a molecular interaction between FGF23 and other factors, including RAAS, we could not examine the detailed mechanisms in the present study. Fifth, our presented model is not a CKD and LVH model as a result of long-term diabetes mellitus, autoimmune disease, or hypertension. However, as mentioned earlier, the coexistence of decreased kidney function and LVH due to increased afterload is a common situation in CKD patients. Therefore, we believe that this model could contribute to the elucidation of the mechanism of the CKD-CVD association. To resolve these issues, we need to plan a further study.

In conclusion, coexisting CKD and LVH further increased serum aldosterone and FGF23 levels and cardiac expression of FGF23 and RAAS-related factors. There was a statistically significantly close correlation of not serum but cardiac FGF23 with LVH and RAAS, suggesting that local FGF23 levels may be associated with RAAS activation and LVH.
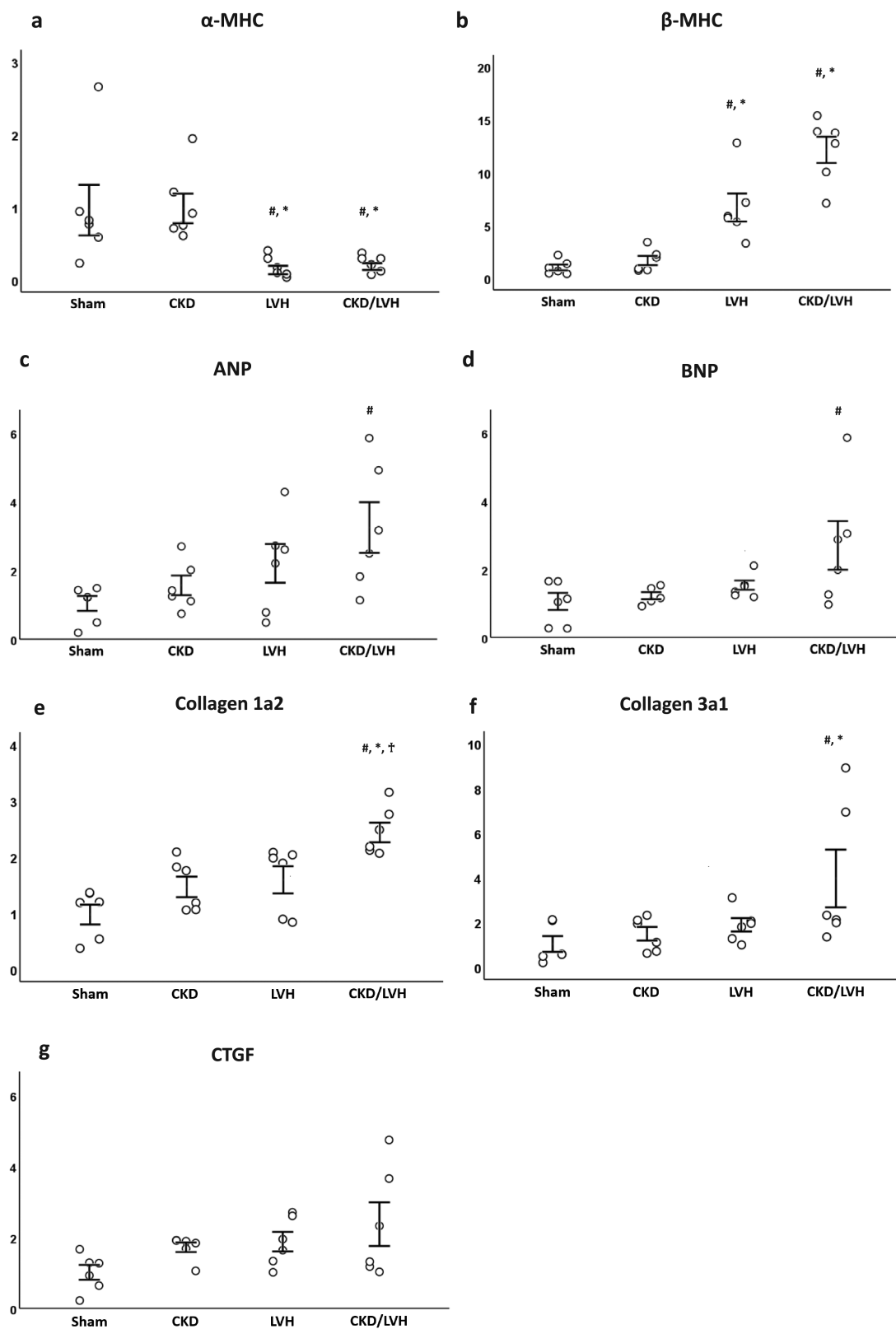
Figure 7. Messenger RNA expressions of cardiac hypertrophy- and cardiac fibrosis-related factors in heart. A, α-myosin heavy chain (α-MHC). B, β-myosin heavy chain (β-MHC). C, Atrial natriuretic peptide (ANP). D, Brain natriuretic peptide (BNP). E, Collagen type I α2 (collagen 1a2). F, Collagen type III α1 (collagen 3a1). G, Connective tissue growth factor (CTGF). Values are expressed as means ± SEM. #vs sham, *P* less than .05; *vs chronic kidney disease (CKD), *P* less than .05; †vs left ventricular hypertrophy (LVH), *P* less than .05.

Table 3. Correlation of fibroblast growth factor 23 and renin-angiotensin-aldosterone system–related factors with cardiac parameters

	HW	rHW	Width	Area	Fibrosis	LVAW	LVPW	FS	EF	cANP	cBNP	cα-MHC	cβ-MHC	cCol1a2	cCol3a1
iFGF23	0.212	0.517[b]	0.617[b]	0.518[b]	0.698[b]	0.449[a]	0.394	−0.639[b]	−0.645[b]	0.329	0.299	−0.181	0.583[b]	0.493[a]	0.528[b]
cFGF23	0.536[b]	0.708[b]	0.641[b]	0.717[b]	0.807[b]	0.726[b]	0.707[b]	−0.816[b]	−0.805[b]	0.399	0.436[a]	−0.512[a]	0.846[b]	0.709[b]	0.445[a]
imFGF23	0.505[a]	0.766[b]	0.649[b]	0.815[b]	0.890[b]	0.728[b]	0.709[b]	−0.820[b]	−0.814[b]	0.403	0.538[b]	−0.569[b]	0.838[b]	0.683[b]	0.487[a]
Ald	0.251	0.641[b]	0.666[b]	0.495[a]	0.616[b]	0.564[b]	0.566[b]	−0.629[b]	−0.625[b]	0.241	0.239	−0.241	0.527[b]	0.500[a]	0.423[a]
cAT1R	0.624[b]	0.765[b]	0.679[b]	0.830[b]	0.768[b]	0.702[b]	0.644[b]	−0.858[b]	−0.863[b]	0.369	0.427[a]	−0.651[b]	0.742[b]	0.555[b]	0.443[a]
cAGT	0.537[b]	0.674[b]	0.730[b]	0.678[b]	0.662[b]	0.779[b]	0.700[b]	−0.692[b]	−0.691[b]	0.490[a]	0.352	−0.703[b]	0.742[b]	0.497[a]	0.473[a]
cACE	0.823[b]	0.784[b]	0.600[b]	0.683[b]	0.628[b]	0.735[b]	0.705[b]	−0.717[b]	−0.714[b]	0.441[a]	0.448[a]	−0.773[b]	0.738[b]	0.457[a]	0.335
cACE2	−0.690[b]	−0.778[b]	−0.613[b]	−0.701[b]	−0.622[b]	−0.752[b]	−0.702[b]	0.714[b]	0.704[b]	−0.528[b]	−0.311	0.803[b]	−0.699[b]	−0.400	−0.226
uAGT	0.485[a]	0.572[b]	0.528[b]	0.557[b]	0.557[b]	0.744[b]	0.694[b]	−0.624[b]	−0.612[b]	0.116	0.213	−0.539[b]	0.683[b]	0.510[a]	0.312
imAng II	0.448[a]	0.656[b]	0.651[b]	0.562[b]	0.637[b]	0.665[b]	0.613[b]	−0.672[b]	−0.676[b]	0.301	0.283	−0.561[b]	0.714[b]	0.389	0.277
imACE	0.700[b]	0.836[b]	0.779[b]	0.853[b]	0.824[b]	0.837[b]	0.821[b]	−0.884[b]	−0.881[b]	0.462[a]	0.561[b]	−0.695[b]	0.834[b]	0.645[b]	0.444[a]
imACE2	−0.690[b]	−0.776[b]	−0.664[b]	−0.586[b]	−0.643[b]	−0.834[b]	−0.794[b]	0.706[b]	0.705[b]	−0.489[a]	−0.476[a]	0.719[b]	−0.786[b]	−0.437[a]	−0.423[a]

Abbreviations: Ald, aldosterone; cα-MHC, cardiac α-myosin heavy chain; cβ-MHC, cardiac β-myosin heavy chain; cACE, cardiac angiotensin-converting enzyme; cACE2, cardiac angiotensin-converting enzyme 2; cAGT, cardiac angiotensinogen; cANP, cardiac atrial natriuretic peptide; cAT1R, cardiac angiotensin II type 1 receptor; cBNP, cardiac brain natriuretic peptide; cCol1a2, cardiac collagen type I α2; cCol3a1, cardiac collagen type III α1; cFGF23, cardiac fibroblast growth factor 23; EF, ejection fraction; FS, fractional shortening; HW, heart weight; iFGF23, intact fibroblast growth factor 23; imACE, immunohistochemical expression of cardiac angiotensin-converting enzyme; imACE2, immunohistochemical expression of cardiac angiotensin-converting enzyme 2; imAng II, immunohistochemical expression of cardiac angiotensin II; imFGF23, immunohistochemical expression of cardiac fibroblast growth factor 23; LVAW, left ventricular anterior wall; LVPW, left ventricular posterior wall; rHW, relative heart weight; uAGT, urinary angiotensinogen.
[a]P less than .05.
[b]P less than .01.

Table 4. Correlation between fibroblast growth factor 23 and renin-angiotensin-aldosterone system–related factors

	Ald	cAT1R	cAGT	cACE	cACE2	uAGT	imAng II	imACE	imACE2
iFGF23	0.388	0.665[b]	0.556[b]	0.285	−0.269	0.164	0.511[a]	0.518[b]	−0.297
cFGF23	0.567[b]	0.780[b]	0.722[b]	0.663[b]	−0.689[b]	0.626[b]	0.713[b]	0.785[b]	−0.666[b]
imFGF23	0.554[b]	0.820[b]	0.762[b]	0.664[b]	−0.623[b]	0.554[b]	0.729[b]	0.862[b]	−0.705[b]

Abbreviations: Ald, aldosterone; cACE, cardiac angiotensin-converting enzyme; cACE2, cardiac angiotensin-converting enzyme 2; cAGT, cardiac angiotensinogen; cAT1R, cardiac angiotensin II type 1 receptor; cFGF23, cardiac fibroblast growth factor 23; iFGF23, intact fibroblast growth factor 23; imAng II, immunohistochemical expression of cardiac angiotensin II; imACE, immunohistochemical expression of cardiac angiotensin-converting enzyme; imACE2, immunohistochemical expression of cardiac angiotensin-converting enzyme 2; imFGF23, immunohistochemical expression of cardiac fibroblast growth factor 23; uAGT, urinary angiotensinogen.
[a]P less than .05.
[b]P less than .01.

Financial Support

Author Contribution

K.O. designed and performed the experiments and wrote the manuscript. H.F. is the guarantor of this work and takes responsibility for the integrity of the data and the accuracy of the data analysis. S.G., K.W., K.K., and S.N. contributed to discussion.

Disclosures

The authors have nothing to disclose.

Data Availability

Some of all data generated or analyzed during this study are included in this published article or in the data repositories listed in "References."

References

1. Gutierrez O, Isakova T, Rhee E, *et al.* Fibroblast growth factor-23 mitigates hyperphosphatemia but accentuates calcitriol deficiency in chronic kidney disease. *J Am Soc Nephrol.* 2005;16(7):2205-2215.
2. Blau JE, Collins MT. The PTH-vitamin D-FGF23 axis. *Rev Endocr Metab Disord.* 2015;16(2):165-174.
3. Gutiérrez OM, Januzzi JL, Isakova T, *et al.* Fibroblast growth factor 23 and left ventricular hypertrophy in chronic kidney disease. *Circulation.* 2009;119(19):2545-2552.
4. Faul C, Amaral AP, Oskouei B, *et al.* FGF23 induces left ventricular hypertrophy. *J Clin Invest.* 2011;121(11):4393-4408.
5. Leifheit-Nestler M, Haffner D. Paracrine effects of FGF23 on the heart. *Front Endocrinol (Lausanne).* 2018;9:278.
6. Slavic S, Ford K, Modert M, *et al.* Genetic ablation of *Fgf23* or *Klotho* does not modulate experimental heart hypertrophy induced by pressure overload. *Sci Rep.* 2017;7(1):11298.
7. Takashi Y, Kinoshita Y, Hori M, Ito N, Taguchi M, Fukumoto S. Patients with FGF23-related hypophosphatemic rickets/osteomalacia do not present with left ventricular hypertrophy. *Endocr Res.* 2017;42(2):132-137.
8. Stöhr R, Schuh A, Heine GH, Brandenburg V. FGF23 in cardiovascular disease: innocent bystander or active mediator? *Front Endocrinol (Lausanne).* 2018;9:351.

9. Mhatre KN, Wakula P, Klein O, *et al.* Crosstalk between FGF23- and angiotensin II-mediated Ca2+ signaling in pathological cardiac hypertrophy. *Cell Mol Life Sci.* 2018;75(23):4403-4416.

10. Feniman De Stefano GM, Zanati-Basan SG, De Stefano LM, *et al.* Aldosterone is associated with left ventricular hypertrophy in hemodialysis patients. *Ther Adv Cardiovasc Dis.* 2016;10(5):304-313.

11. Stein AB, Goonewardena SN, Jones TA, *et al.* The PTIP-associated histone methyltransferase complex prevents stress-induced maladaptive cardiac remodeling. *PLoS One.* 2015;10(5):e0127839.

12. Kilkenny C, Browne WJ, Cuthill IC, Emerson M, Altman DG. Improving bioscience research reporting: the ARRIVE guidelines for reporting animal research. *PLoS Biol.* 2010;8(6):e1000412.

13. McGrath JC, Drummond GB, McLachlan EM, Kilkenny C, Wainwright CL. Guidelines for reporting experiments involving animals: the ARRIVE guidelines. *Br J Pharmacol.* 2010;160(7):1573-1576.

14. Siragy HM, Carey RM. Role of the intrarenal renin-angiotensin-aldosterone system in chronic kidney disease. *Am J Nephrol.* 2010;31(6):541-550.

15. Lang F, Leibrock C, Pandyra AA, Stournaras C, Wagner CA, Föller M. Phosphate homeostasis, inflammation and the regulation of FGF-23. *Kidney Blood Press Res.* 2018;43(6):1742-1748.

16. Lei B, Chess DJ, Keung W, O'Shea KM, Lopaschuk GD, Stanley WC. Transient activation of p38 MAP kinase and up-regulation of Pim-1 kinase in cardiac hypertrophy despite no activation of AMPK. *J Mol Cell Cardiol.* 2008;45(3):404-410.

17. Zhang M, Takimoto E, Lee DI, *et al.* Pathological cardiac hypertrophy alters intracellular targeting of phosphodiesterase type 5 from nitric oxide synthase-3 to natriuretic peptide signaling. *Circulation.* 2012;126(8):942-951.

18. Rockman HA, Wachhorst SP, Mao L, Ross J Jr. ANG II receptor blockade prevents ventricular hypertrophy and ANF gene expression with pressure overload in mice. *Am J Physiol.* 1994;266(6 Pt 2):H2468-H2475.

19. Fujii H, Joki N. Mineral metabolism and cardiovascular disease in CKD. *Clin Exp Nephrol.* 2017;21(Suppl 1):53-63.

20. Vogt I, Haffner D, Nestler ML. FGF23 and phosphate–cardiovascular toxins in CKD. *Toxins (Basel).* 2019; 11(11):647.

21. Smith ER, Holt SG, Hewitson TD. αKlotho-FGF23 interactions and their role in kidney disease: a molecular insight. *Cell Mol Life Sci.* 2019;76(23):4705-4724.

22. Mirza MA, Larsson A, Melhus H, Lind L, Larsson TE. Serum intact FGF23 associate with left ventricular mass, hypertrophy and geometry in an elderly population. *Atherosclerosis.* 2009;207(2):546-551.

23. Grabner A, Amaral AP, Schramm K, *et al.* Activation of cardiac fibroblast growth factor receptor 4 causes left ventricular hypertrophy. *Cell Metab.* 2015;22(6):1020-1032.

24. Matsui I, Oka T, Kusunoki Y, *et al.* Cardiac hypertrophy elevates serum levels of fibroblast growth factor 23. *Kidney Int.* 2018;94(1):60-71.

25. Fujii H, Watanabe K, Kono K, Goto S, Watanabe S, Nishi S. Changes in serum and intracardiac fibroblast growth factor 23 during the progression of left ventricular hypertrophy in hypertensive model rats. *Clin Exp Nephrol.* 2019;23(5):589-596.

26. Mitsnefes MM, Betoko A, Schneider MF, *et al.* FGF23 and left ventricular hypertrophy in children with CKD. *Clin J Am Soc Nephrol.* 2018;13(1):45-52.

27. Radloff J, Pagitz M, Andrukhova O, Oberbauer R, Burgener IA, Erben RG. Aldosterone is positively associated with circulating FGF23 levels in chronic kidney disease across four species, and may drive FGF23 secretion directly. *Front Physiol.* 2021;12:649921.

28. Böckmann I, Lischka J, Richter B, *et al.* FGF23-mediated activation of local RAAS promotes cardiac hypertrophy and fibrosis. *Int J Mol Sci.* 2019; 20(18):4634.

29. Pi M, Ye R, Han X, *et al.* Cardiovascular interactions between fibroblast growth factor-23 and angiotensin II. *Sci Rep.* 2018;8(1):12398.

30. Zhang B, Umbach AT, Chen H, *et al.* Up-regulation of FGF23 release by aldosterone. *Biochem Biophys Res Commun.* 2016;470(2):384-390.

31. Leifheit-Nestler M, Kirchhoff F, Nespor J, *et al.* Fibroblast growth factor 23 is induced by an activated renin-angiotensin-aldosterone system in cardiac myocytes and promotes the pro-fibrotic crosstalk between cardiac myocytes and fibroblasts. *Nephrol Dial Transplant.* 2018;33(10):1722-1734.

32. Shimada T, Hasegawa H, Yamazaki Y, *et al.* FGF-23 is a potent regulator of vitamin D metabolism and phosphate homeostasis. *J Bone Miner Res.* 2004;19(3):429-435.

33. Li YC, Kong J, Wei M, Chen ZF, Liu SQ, Cao LP. 1,25-Dihydroxyvitamin D(3) is a negative endocrine regulator of the renin-angiotensin system. *J Clin Invest.* 2002;110(2):229-238.

34. Chen S, Law CS, Grigsby CL, *et al.* Cardiomyocyte-specific deletion of the vitamin D receptor gene results in cardiac hypertrophy. *Circulation.* 2011;124(17):1838-1847.

35. Fujii H, Nakai K, Yonekura Y, *et al.* The vitamin D receptor activator maxacalcitol provides cardioprotective effects in diabetes mellitus. *Cardiovasc Drugs Ther.* 2015;29(6):499-507.

36. Santos RAS, Ferreira AJ, Verano-Braga T, Bader M. Angiotensin-converting enzyme 2, angiotensin-(1-7) and Mas: new players of the renin-angiotensin system. *J Endocrinol.* 2013;216(2):R1-R17.

37. Burns KD. The emerging role of angiotensin-converting enzyme-2 in the kidney. *Curr Opin Nephrol Hypertens.* 2007;16(2):116-121.

38. Crackower MA, Sarao R, Oudit GY, *et al.* Angiotensin-converting enzyme 2 is an essential regulator of heart function. *Nature.* 2002;417(6891):822-828.

39. Bodiga S, Zhong JC, Wang W, *et al.* Enhanced susceptibility to biomechanical stress in ACE2 null mice is prevented by loss of the p47(phox) NADPH oxidase subunit. *Cardiovasc Res.* 2011;91(1):151-161.

40. Oudit GY, Kassiri Z, Patel MP, *et al.* Angiotensin II-mediated oxidative stress and inflammation mediate the age-dependent cardiomyopathy in ACE2 null mice. *Cardiovasc Res.* 2007;75(1):29-39.

41. Dai B, David V, Martin A, *et al.* A comparative transcriptome analysis identifying FGF23 regulated genes in the kidney of a mouse CKD model. *PLoS One.* 2012;7(9):e44161.

42. Anguiano L, Riera M, Pascual J, *et al*; NEFRONA study. Circulating angiotensin-converting enzyme 2 activity in patients with chronic kidney disease without previous history of cardiovascular disease. *Nephrol Dial Transplant.* 2015;30(7):1176-1185.

43. Sousa AGP, de Sousa Cabral JV, El-Feghaly WB, de Sousa LS, Nunes AB. Hyporeninemic hypoaldosteronism and diabetes mellitus: pathophysiology assumptions, clinical aspects and implications for management. *World J Diabetes.* 2016;7(5):101-111.

44. Remuzzi G, Perico N, Macia M, Ruggenenti P. The role of renin-angiotensin-aldosterone system in the progression of chronic kidney disease. *Kidney Int Suppl.* 2005;68(99):S55-S65.